Enzyme and Microbial Technology 191 (2025) 110709

Contents lists available at ScienceDirect

Enzyme and Microbial Technology

journal homepage: www.elsevier.com/locate/enzmictec

Modulating dioxygenase and hydroperoxide isomerase activities in *Burkholderia thailandensis* lipoxygenase

Ruth Chrisnasari [a,b,c], Roelant Hilgers [a], Guanna Li [d], Jean-Paul Vincken [a], Willem J.H. van Berkel [a], Marie Hennebelle [a], Tom A. Ewing [b,*]

[a] Laboratory of Food Chemistry, Wageningen University & Research, Bornse Weilanden 9, Wageningen 6708 WG, the Netherlands
[b] Wageningen Food & Biobased Research, Wageningen University & Research, Bornse Weilanden 9, Wageningen 6708 WG, the Netherlands
[c] Faculty of Biotechnology, University of Surabaya (UBAYA), Surabaya 60293, Indonesia
[d] Biobased Chemistry & Technology, Wageningen University & Research, Bornse Weilanden 9, Wageningen 6708 WG, the Netherlands

ARTICLE INFO

Keywords:
Epoxy alcohol
Hydroperoxide
Hydroperoxide isomerase
Ketone
Lipoxygenase

ABSTRACT

Lipoxygenases (LOXs) are enzymes that catalyze the regioselective dioxygenation of polyunsaturated fatty acids (PUFAs), leading to the formation of fatty acid hydroperoxides (FAHPs). In addition to dioxygenase activity, some eukaryotic LOXs exhibit hydroperoxide isomerase (HPI) activity under specific conditions, resulting in the production of structurally diverse compounds such as epoxy alcohols and ketones. Until now, the presence of HPI activity in bacterial LOXs has not been documented. In this study, we investigated the HPI activity of LOX from *Burkholderia thailandensis* (Bt-LOX) and examined the effects of reaction conditions on its catalytic profile using three different C18 PUFA substrates. The results demonstrated that Bt-LOX exhibits significant HPI activity, especially at high enzyme concentrations, with ketone formation showing strong substrate dependence. Oxygen level was identified as a critical factor in directing the catalytic performance of Bt-LOX: HPI activity was inhibited under O_2-saturated conditions and enhanced under O_2-limited conditions. These findings establish Bt-LOX as the first bacterial LOX reported to exhibit pronounced HPI activity, and highlights its expanded potential for biocatalytic applications.

1. Introduction

Lipoxygenases (LOXs; EC 1.13.11.x) are non-heme iron (or, in some cases, manganese) dependent enzymes that catalyze the regioselective dioxygenation of polyunsaturated fatty acids (PUFAs), producing fatty acid hydroperoxides (FAHPs). The non-heme iron of LOX exists in two oxidation states: ferrous (Fe^{2+}) and ferric (Fe^{3+}) [1]. Newly isolated enzymes are typically in the ferrous state, which is inactive towards PUFAs. They require a priming reaction with FAHPs to convert the iron to its ferric state [2,3], thereby, activating the enzyme to enter the dioxygenase catalytic cycle [4]. An alkoxyl radical or epoxy-allylic radical is postulated as an intermediate in the LOX activation process [5,6]. The radical intermediate subsequently dissociates through an oxygen-dependent dissociation process, leading to the formation of epoxy-allylic hydroperoxides, which are then further transformed into epoxy-allylic ketones [5]. LOX activation is a single turnover event, meaning that once the enzyme is oxidized to its ferric form, it will remain in this form and no longer react with FAHPs [1].

An exception applies to certain eukaryotic LOXs that exhibit hydroperoxide isomerase (HPI) activity [5–8]. These enzymes, in their ferrous form, can convert FAHPs into epoxy alcohols or ketones, reverting to their ferrous state after product release [5,6]. Despite the fact that the ketone is not an isomer of the FAHP, both epoxy alcohols and ketones are considered as HPI products [6]. The formation of an epoxy alcohol or ketone via the HPI activity of LOX involves several key steps [6] (Fig. 1). First, the ferrous enzyme (LOX–Fe^{2+}) catalyzes the homolytic cleavage of the hydroperoxide O–O bond, generating an alkoxy radical intermediate. Concurrently, the hydroxyl group from the hydroperoxide is transferred to the enzyme, forming a LOX–Fe^{3+}–OH complex. Next, the alkoxy radical intermediate can cyclize to form an epoxyallylic radical, and the two species may exist in equilibrium. The final step proceeds through one of two proposed pathways [6]. In one pathway, the alkoxy radical undergoes C–H bond scission (likely via a hydrogen atom transfer) to produce a fatty acid ketone and water, which regenerates LOX–Fe^{2+}. In the other pathway, the hydroxyl group in the LOX–Fe^{3+}–OH complex rebounds to the epoxyallylic radical

* Corresponding author.
E-mail address: tom.ewing@wur.nl (T.A. Ewing).

https://doi.org/10.1016/j.enzmictec.2025.110709
Received 26 May 2025; Received in revised form 3 July 2025; Accepted 7 July 2025
Available online 8 July 2025

intermediate, resulting in the formation of an epoxy alcohol and restoring LOX–Fe^{2+}.

The presence of HPI activity in LOXs is of interest because the resulting fatty acid epoxy alcohols or ketones may have unique properties. Typically, the hydroxy, epoxy or keto group impart special characteristics to fatty acids, such as higher viscosity and reactivity [9]. Due to their distinctive chemical properties, these fatty acid derivatives can be used in a wide range of products, including resins, waxes, nylons, plastics, corrosion inhibitors, cosmetics, and coatings [9]. Moreover, unsaturated epoxy alcohols serve as potent starting materials for the synthesis of biologically active molecules [10], such as hepoxilins [11,12], trioxilins [12] and leukotrienes.

The HPI activity of LOX has generally been observed only under specific conditions. For example, soybean LOX-1 exhibits HPI activity in the presence of excess FAHP and under anaerobic conditions [7,13]. In manganese LOX from the fungus *Gaeumannomyces avenae*, the G316A mutation induces HPI activity by altering oxygen disposition in the active site [8]. Notable HPI activity has also been identified in an unusual human epidermal LOX3, which catalyzes dioxygenase activity with a long lag phase, requiring high concentrations of a hydroperoxide activator [14]. Moreover, in human epidermal LOX3, pronounced HPI activity was observed under limited oxygen supply [5]. The dual functionality of dioxygenase and HPI activity makes these LOXs versatile biocatalysts; however, it also presents challenges, complicating product purification. Therefore, maximizing the application potential of LOXs requires a deeper understanding of how to steer their reactions toward either dioxygenase or HPI activity, depending on the desired outcome.

Currently, there is limited information regarding the occurrence of HPI activity in other LOXs, particularly those of bacterial origin. Bacterial LOXs are gaining attention due to their high activity [15] and ability to catalyze reactions on a broad spectrum of PUFAs with distinct regioselectivity [16]. Among these bacterial enzymes, LOX from *Burkholderia thailandensis* (Bt-LOX) was previously shown to display high activity toward various PUFAs (C18–C22), with regioselectivity preferentially targeting the ω−5 position [17]. Building upon this foundation, this study investigates the presence of HPI activity in Bt-LOX and evaluates how reaction conditions influence its catalytic behavior. Key parameters such as enzyme concentration, incubation time, and oxygen availability were systematically analyzed across three different C18 PUFA substrates. Increased enzyme concentrations were hypothesized to enhance HPI activity by providing more ferrous enzyme for catalysis, while extended incubation times were expected to facilitate product accumulation. Moreover, modulating oxygen levels was predicted to direct the reaction pathway, as HPI activity is often associated with anaerobic or oxygen-limited conditions [5,7,13]. Elucidating these factors allows for precise control over Bt-LOX's dual activities, unlocking its potential for targeted biocatalytic applications and expanding its utility in chemical synthesis.

2. Materials and methods

2.1. Materials

The gene for *Burkholderia thailandensis* lipoxygenase (Bt-LOX) (NCBI ABC36974.1), optimized for expression in *Escherichia coli*, was obtained from GenScript Biotech in Rijswijk, The Netherlands. This gene was inserted into a pET-19b plasmid (Novagen, USA) using the *Nde*I and BlpI restriction sites. To facilitate protein purification via metal affinity chromatography, a 10x His-Tag and an enterokinase site were added to the enzyme's N-terminus. The materials for enzyme production and purification were sourced as follows: *E. coli* BL21(DE3) competent cells from Invitrogen, California, USA; Luria Bertani medium, pepstatin A, and ampicillin sodium salt from Sigma-Aldrich, Missouri, USA; Isopropyl β-D-1-thiogalactopyranoside (IPTG) from Duchefa Biochemie B.V., Haarlem, The Netherlands; BugBuster master mix and Ni-NTA His-bind resin from Millipore-Merck, Darmstadt, Germany; cOmplete mini EDTA-free protease inhibitor cocktail from Roche, Mannheim, Germany; and VivaSpin from GE Healthcare, Buckinghamshire, UK.

Chemicals for enzymatic assays and product analysis were obtained from the following sources: linoleic acid (LA; C18:2 Δ9*Z*,12*Z*), α-linolenic acid (ALA; C18:3 Δ9*Z*,12*Z*,15*Z*) and γ-linolenic acid (GLA; C18:3 Δ6*Z*,9*Z*,12*Z*) were sourced from Nu-Chek Prep, Inc., Minnesota, USA. Standards for FAHPs, including 13(*S*)-Hydroperoxy-9*Z*,11*E*-octadecadienoic acid (13-HPODE) and 13(*S*)-Hydroperoxy-9*Z*,11*E*,15*Z*-octadecatrienoic acid (13-HPOTrE), as well as some potential FAHP derivative products including 13*S*-hydroxy-9*Z,11E*-octadecadienoic acid (13-HOTE), 13-oxo-9*Z*,11*E*-octadecadienoic acid (13-OxoODE), cis-12(13)-epoxy-9*Z*-octadecenoic acid (12(13)-EpOME), 13-oxo-9*Z*,11*E*,15*Z*-octadecatrienoic acid (13-OxoOTrE), and *cis*-12(13)-epoxy-9*Z*,15*Z*-octadecadienoic acid (12(13)-EpODE) were acquired from Larodan, Solna, Sweden. Ethyl acetate, methanol absolute and acetonitrile, all in ULCMS grade were purchased from Biosolve B.V., Valkenswaard, The Netherlands.

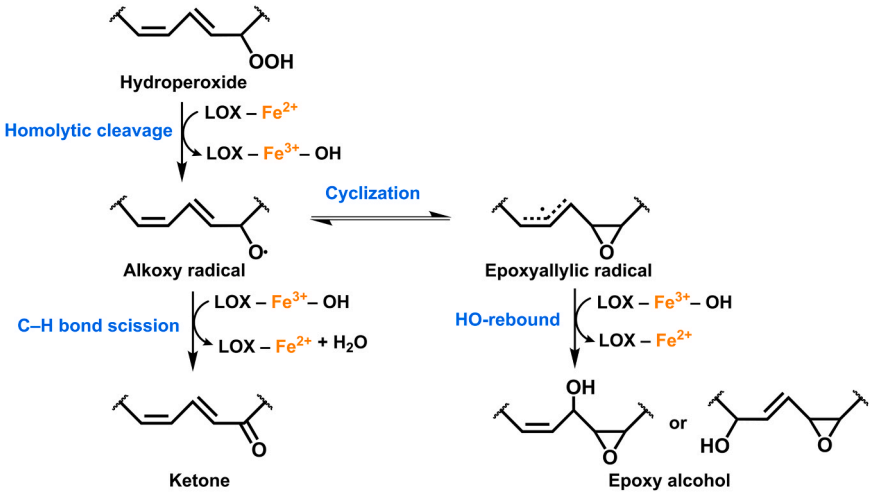

Fig. 1. Proposed hydroperoxide isomerase catalytic mechanism of lipoxygenase [5,6]. The reaction includes several key steps: (i) Homolytic cleavage of the hydroperoxide O–O bond by a ferrous enzyme to form an alkoxy radical; (ii) Cyclization of the alkoxy radical to an epoxyallylic radical, and the two species may exist in equilibrium; (iii) The alkoxy radical undergoes C–H bond scission to produce a fatty acid ketone and water, which regenerates LOX–Fe^{2+}. Alternatively, the hydroxyl group in the LOX–Fe^{3+}–OH complex rebounds to the epoxyallylic radical intermediate, resulting in the formation of an epoxy alcohol and restoring LOX–Fe^{2+}.

2.2. Protein expression and purification

Protein expression and purification were done according to the previously reported protocol [17]. Recombinant *E. coli* BL21(DE3) carrying the pET-19b_Bt-LOX plasmid was grown in Luria Bertani medium at 37 °C with continuous shaking at 250 rpm. The empty pET-19b plasmid was used as a control for protein overexpression. Upon reaching an optical density of 0.6 −0.8 at 600 nm (OD600), 0.5 mM Isopropyl β-*D*-1-thiogalactopyranoside (IPTG) was added. Afterwards, the culture was incubated at 16 °C with shaking at 150 rpm for 48 h. Subsequently, cells were harvested by centrifugation at 7000×*g* for 15 min at 4 °C and stored at −20 °C until protein purification.

To purify Bt-LOX, frozen cell pellets from a 200 mL culture were resuspended in a lysis solution and incubated on a slow-setting rotating mixer for 20 min at room temperature. The lysis solution consisted of one Mini EDTA-free cOmplete protease inhibitor cocktail tablet and 1 μM pepstatin A dissolved in 10 mL of BugBuster Master Mix. After incubation, the mixture was centrifuged at 16,000×*g* for 20 min at 4 °C to remove cell debris and the resulting supernatant was filtered through a 0.22 μm membrane filter. Purification was then carried out using a gravity flow column packed with 1 mL of Ni-NTA His-bind resin. Prior to sample application, the column was equilibrated with 10 column volumes (CV) of an equilibration buffer composed of 50 mM NaH_2PO_4, 300 mM NaCl, and 10 mM imidazole at pH 7.0. The filtered supernatant was applied to the column, followed by washing with 2 CV each of four washing buffers at pH 7.0, containing 50 mM NaH_2PO_4, 300 mM NaCl, and increasing concentrations of imidazole (20, 50, 100, and 150 mM, respectively). Elution of the purified enzyme was achieved using 4 CV of elution buffer at pH 7.0, containing 50 mM NaH_2PO_4, 300 mM NaCl, and 250 mM imidazole. Concentration and desalting of elution fractions were performed using a VivaSpin spin filter with a molecular weight cut-off of 10 kDa, and the enzyme was stored in 100 mM Bis-Tris buffer at pH 6.0. Protein content was determined using Bradford assay [18]. The specific activity of the purified enzyme was 36.8 U/mg. One unit of enzyme activity (U) is defined as the amount of enzyme that produces 1 μmol of hydroperoxide per minute using LA as the substrate at 30 °C and pH 6.0. The specific activity was calculated based only on the holoenzyme, taking the enzyme's iron load into account [17].

2.3. Preparation of substrate stock solutions

PUFAs were solubilized and freshly prepared according to a previously reported protocol [19]. In a 10 mL volumetric flask, PUFA (LA, ALA or GLA) was mixed with 12.5 μL of Tween-20 in 4 mL milli-Q water. After adding 0.55 mL of 0.5 M NaOH, the mixture became clear, and milli-Q water was added to adjust the volume to 10 mL, resulting in a final PUFA concentration of 4.33 mM.

2.4. Effect of enzyme concentration and reaction time on HPI activity of Bt-LOX

To investigate the effect of enzyme concentration and reaction time on HPI activity of Bt-LOX, three different C18 PUFA substrates were used, i.e., LA, ALA, and GLA. For the examination of the effect of enzyme concentration, 10, 20, or 30 μL of 308 μg/mL Bt-LOX and 240 μL of 4.33 mM PUFA were diluted to a total volume of 1.0 mL with 100 mM Bis-Tris buffer pH 6.0. This resulted in final enzyme concentration of 3, 6, or 9 μg/mL, respectively, and a substrate concentration of 1.04 mM. Negative control reactions (without enzyme) for each substrate were prepared using an equivalent amount of substrate diluted with 760 μL 100 mM Bis-Tris buffer at pH 6.0. The reaction mixtures were then incubated for 30 min at 30 °C with agitation at 300 rpm. After incubation, the reaction mixture was transferred to a Kimax tube containing 5 mL of ethyl acetate and briefly vortexed to stop the enzymatic reaction and extract the lipid fractions [20]. The mixture was subsequently centrifuged at 5000×*g* for 15 min at room temperature, resulting in the separation of three layers: an aqueous phase at the bottom, denatured protein at the interlayer, and an organic phase at the top. Following centrifugation, 4 mL of the upper layer was collected and evaporated under a nitrogen flow at 30 °C. Once the ethyl acetate had completely evaporated, the sample was diluted in 4 mL of methanol and stored at −80 °C until further analysis.

To assess the effect of incubation time on HPI activity of Bt-LOX, 10 μL of 309 μg/mL Bt-LOX and 240 μL of 4.33 mM PUFA were diluted to a total volume of 1.0 mL with 100 mM Bis-Tris buffer pH 6.0, resulting in a final enzyme concentration of 3 μg/mL and a substrate concentration of 1.04 mM. These mixtures were incubated at 30 °C for 0, 30, 60, 90 and 120 min, respectively. Negative control reactions (without enzyme) for each substrate were prepared using an equivalent amount of substrate diluted with 760 μL 100 mM Bis-Tris buffer at pH 6.0 and incubated simultaneously with the enzyme samples. To make sure that FAHP is stable under the experimental conditions applied, 100 μL of 295 μM standard 13-HPOTrE was added to 900 μL 100 mM Bis-Tris buffer pH 6.0 and incubated in the same way as zero and 120 min time samples. After incubation, the lipid fractions from enzymatic reactions, negative controls, and standard samples were extracted using the same protocol as described above. The experiments for both the effect of enzyme concentrations and reaction times were done in two biological replicates.

2.5. Effect of oxygen level on HPI activity of Bt-LOX

To evaluate the effect of oxygen level on HPI activity of Bt-LOX, the buffer used for enzymatic reactions was saturated with O_2 (for O_2-saturated conditions) or N_2 (for O_2-limited conditions) by bubbling it with the corresponding gas flow for at least 3 h prior enzymatic reaction. The enzyme and the substrates stock solutions were neither flushed with O_2 nor N_2. The enzymatic reaction was conducted in a greenhouse plus parallel synthesizer from Radley, Essex, UK. Prior to the enzymatic reaction, the chamber of the parallel synthesizer was saturated with O_2 (for O_2-saturated conditions) or N_2 (for O_2-limited conditions) flow for 30 min. The enzymatic reaction consisted of 30 μL of 298 μg/mL Bt-LOX, 100 μL of 4.33 mM PUFA (i.e., LA and ALA) and 870 μL of 100 mM Bis-Tris buffer pH 6.0, resulting in a final enzyme concentration of 9 μg/mL and a substrate concentration of 433 μM. These mixtures were incubated at 30 °C for 60 min under O_2 (for O_2-saturated conditions) or N_2 (for O_2-limited conditions) flow of 100 mL/min. Negative control reactions (without enzyme) for each substrate were prepared using an equivalent amount of substrate diluted with 900 μL 100 mM Bis-Tris buffer at pH 6.0. The negative control reactions were incubated under the same conditions as and simultaneously to the enzyme samples. After incubation, the lipid fractions were extracted using the same protocol as described above. The experiment was done in three replicates.

2.6. Product characterization using RP-UHPLC-PDA-HRMS

The enzymatic reaction products were analyzed using a Thermo Vanquish UHPLC system (Thermo Fisher Scientific, Pittsburgh, PA, USA) equipped with a reversed-phase (RP) Acquity UPLC BEH C18 column (2.1 ×150 mm, 1.7 μm particle size; Waters Corporation, Milford, MA, USA), a photodiode array detector (PDA), and a Thermo Q Exactive Focus Hybrid Quadrupole-Orbitrap Fourier Transform mass spectrometer (FTMS) (Thermo Fisher Scientific, Pittsburgh, PA, USA). The autosampler was kept at 10 °C. The analysis was conducted with a flow rate of 350 μL/min, and the column was maintained at 25 °C. The mobile phase consisted of ultrapure water with 0.01 % acetic acid (Phase A) and acetonitrile with 0.01 % acetic acid (Phase B). The elution program began with 50 % B from 0 to 1.25 min, followed by a linear gradient to 90 % B from 1.25 to 51.43 min, and then increased to 100 % B from 51.43 to 52.68 min. The solvent was held at 100 % B from 52.68 to 58.90 min, then reduced to 50 % B from 58.90 to 60.21 min, and finally

maintained at 50 % B from 60.21 to 66.48 min for equilibration. The high-resolution mass spectrometer (HRMS) with a Heated Electrospray Ionization (HESI) probe operated in negative ionization mode, with a capillary temperature of 250°C, an ion spray voltage of 2.5 kV, and a sheath gas flow rate of 45 psi. Full MS data were collected in discovery mode at a resolution of 70,000 over an *m/z* range of 250–1000. Additionally, Higher-energy Collisional Dissociation (HCD) fragmentation data were obtained with normalized collision energy of 45 %. Data processing was performed using Xcalibur 4.5 (Thermo Fisher Scientific).

The identification of products from the dioxygenation activity of Bt-LOX involved analyzing peaks with specific *m/z* values corresponding to the mass of derived FAHPs from each PUFA. The FAHP peaks were confirmed by measuring their absorbance at 234 nm to detect the presence of a conjugated diene moiety [21]. The position of the hydroperoxide in FAHPs was determined based on diagnostic HCD fragments resulting from the cleavage of the C–C bond near the hydroperoxide group [22,23]. Epoxy alcohols and ketones were identified by analyzing peaks with specific *m/z* values corresponding to these compounds derived from each PUFA. The fragmentation patterns of these peaks were then evaluated. Epoxy alcohols were confirmed by analyzing the diagnostic HCD fragments resulting from the cleavage of the C-C bond near the epoxide and hydroxyl groups, respectively [5]. Ketones were confirmed by comparing their retention time (RT) and fragmentation pattern with those of standard compounds (13-OxoODE and 13-OxoOTrE). Other ketone regioisomers (e.g., 9-oxoODE and 9-oxoOTrE) were identified by assessing fragments resulting from similar cleavage patterns as their regio-isomers. Additionally, ketones were further confirmed by measuring their absorbance at 282 nm [8].

2.7. Structure modelling and docking of FAHPs at the binding pocket of Bt-LOX

The three-dimensional structure of Bt-LOX was modeled using AlphaFold2 with the casp14 settings [24]. Please note that this study was conducted before the release of AlphaFold3 [25]. However, a subsequent structural comparison between the AlphaFold2 and AlphaFold3 models of Bt-LOX (Fig. S1) indicated no significant differences in the structures of the core domain and identical positioning of the iron atom. To visualize how the FAHPs bind within the substrate binding pocket of Bt-LOX, molecular docking simulation was performed using Molecular Operating Environment (MOE) version 2022.02 (Chemical Computing Group, Montreal, QC, Canada). The structures of FAHPs were obtained from PubChem to create a library in MOE. Structural preparation of FAHPs involved energy minimization and adjustment of protonation/deprotonation states. The Amber10:EHT forcefield with default setting of MOE was used for energy minimization. Before the docking process, iron was added to the Alphafold model of Bt-LOX. The position of the iron was confirmed by comparing the docking results to the position of the iron in *P. aeruginosa* LOX (PDB: 5IR5). The iron was then adjusted for valency, and the Bt-LOX-Fe structure was energy minimized and prepared by setting the pH to 6.0, ionic strength to 100 mM, and temperature to 25 °C. Determination of iron-coordinating residues was performed by selecting the corresponding residues that were found to be coordinated to iron in *P. aeruginosa* LOX (PDB: 5IR5, sequence identity 49.6 %). The prepared PUFAs were subsequently docked to the residues coordinating with iron (H388, H393, H565, N569, and I685) using triangle matcher placement and induced fit refinement settings. Scoring was based on London dG scoring, with a more negative S-score indicating increased binding affinity between FAHPs and LOX. The docking process was conducted in triplicate, with each replicate collecting 30 poses, and the 5 poses with the lowest S-scores were evaluated. Docked poses were selected based on specific criteria, including the lowest S-score, Root Mean Square Deviation (RMSD) ≤ 2, and the proximity of the hydroperoxide group to the iron.

2.8. Quantum mechanics/molecular mechanics (QM/MM) calculations

Combined QM and MM calculations were applied using the two-level ONIOM methodology as implemented in Gaussian 16 B.01 [26]. Input structures were prepared starting from Bt-LOX with either 13-HPODE or 13-αHPOTrE docked in the substrate binding pocket (see previous section). The complete enzyme-substrate systems were then trimmed to only include amino acid residues within a 15 Å radius sphere around the iron atom. Subsequently, all free (i.e., not covalently bound) amino acid residues in the outer layer of the system, resulting from the trimming, were removed. Amino acids at the border of the system were protonated to avoid unpaired electron density at the edge of the system (Fig. 2A). In all ALA derivatives, the terminal CH_3 group was removed to further reduce the size of the system. To obtain starting conformations of fatty acid alkoxy and epoxyallylic radicals, the O–O bonds of 13-HPODE and 13-αHPOTrE were manually cleaved, and the resulting free OH radical was placed next to the iron atom to obtain an Fe–O distance of ~1.8 Å. The starting conformations of the epoxy alcohol and ketone were obtained from the optimized geometries of the epoxyallylic and alkoxy radicals, respectively. To generate the epoxy alcohol, the OH ligand was manually transferred from the iron atom to the C atom adjacent to the epoxy group (i.e., C11). To obtain the ketone, both the OH ligand of the iron atom and the H atom of C13 were removed. The energy of the resulting H_2O molecule was calculated separately. In all calculations, the iron atom, fatty acid derivatives, and the side chains of the coordinating amino acid residues (i.e., His388, His393, His565, Asn569 and Ile695) were included in the QM region (Fig. 2B). The rest of the system was included in the MM region. The QM region was optimized using the ωB97xD functional, using the LANL2DZ basis set for Fe, and the 6–311 G (d,p) basis set for all other atoms. The MM region was described by the UFF force field [26]. In all structures, a high-spin iron atom was assumed, based on previous observations [27,28].

3. Results and discussion

HPI activity has been reported in a few LOXs from different kingdoms [5–8], but it has not been documented in bacterial LOX. Here, we investigated whether bacterial LOX from *Burkholderia thailandensis* (Bt-LOX) exhibits HPI activity by examining the effects of enzyme concentration, incubation time, and oxygen level on its catalytic profile using three different C18 PUFA substrates.

3.1. Effect of enzyme concentration on HPI activity

The effect of enzyme concentration on the HPI activity of Bt-LOX was investigated using three different concentrations: 3, 6, and 9 μg/mL. A reaction without enzyme addition was included as a control. The reaction products were analyzed using RP-UHPLC-PDA-HRMS, and the chromatograms are shown in Fig. 3. The retention times (RT) of the resulting products, along with their parent ions and diagnostic fragments in MS^2 spectra used for identification, are listed in Table S1.

The results showed that Bt-LOX produces 13-HPODE (RT 12.95), 13-αHPOTrE (RT 9.92), and 13-γHPOTrE (RT 10.32) as the main FAHP products of dioxygenase activity from LA, ALA, and GLA, respectively. Examples of MS/MS spectra for dioxygenation regioselectivity determination based on diagnostic fragments are provided in Fig. S2.

Epoxy alcohols, specifically 12(13)-epoxy-11-hydroxy-octadec-9-enoic acid (12(13)-Ep,11-HOME) (RT 5.82), 12(13)-epoxy-11-hydroxy-octadec-9,15-dienoic acid (12(13)-Ep,11-αHODE) (RT 4.46), and 12(13)-epoxy-11-hydroxy-octadec-6,9-dienoic acid (12(13)-Ep,11-γHODE) (RT 4.97), were detected as the products of HPI activity from LA, ALA, and GLA, respectively. Examples of MS/MS spectra for identification of epoxy alcohols based on diagnostic fragments are provided in Fig. S3. Moreover, multiple epoxy alcohol isomers were observed for all three substrates, as shown in Fig. S4. The chromatograms for ALA and GLA suggest the formation of diastereomers, based on their identical

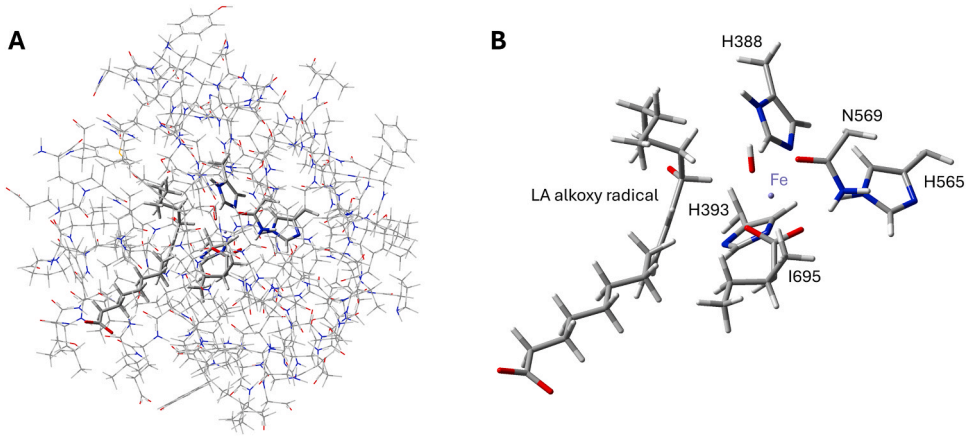

Fig. 2. QM and MM region (A) and a close-up of the QM region (B) of the Bt-LOX model used in QM/MM calculations, in this example containing the LA alkoxy radical as a bound intermediate. Illustrations of QM and MM regions containing other substrates are provided in the Supporting Information. Structures within the QM region are shown as tubes, and structures in the MM region are shown as wireframe.

MS/MS spectra (Table S1). Notably, the chromatographic profiles indicate a clear predominance of one diastereomer, suggesting that the enzymatic reaction favors the formation of a specific stereoisomer.

To determine whether Bt-LOX produces ketones from its HPI activity, the chromatograms of enzymatic reaction products were compared to those of ketone standards (i.e., 13-Oxo-ODE and 13-Oxo-OTrE), as shown in Fig. S5. Ketones were observed to elute at nearly the same retention time (RT) as their corresponding FAHPs, 13-HPODE and 13-HPOTrE, respectively (Fig. S5). Since the full MS spectra of FAHPs display both the *m/z* values of intact FAHPs and their dehydrated forms (which match the *m/z* values of the corresponding ketones), ketone identification was conducted by comparing extracted ion chromatograms of the *m/z* values of ketones and of intact FAHPs. Based on the comparison of these extracted ion chromatograms (Fig. 4), ketones were barely detected when LA was used as the substrate, even at the highest enzyme concentration, as indicated by the identical peak shapes of the *m/z* values 293.2126 (13-Oxo-ODE) and 311.2231 (13-HPODE). When GLA was used as the substrate, a shoulder peak of *m/z* 291.1973 (13-Oxo-γOTrE) was observed at higher enzyme concentrations (≥6 μg/mL), indicating that a ketone (13-Oxo-γOTrE) coeluted with FAHP (13-γHPOTrE). Similar to the observations with GLA, when ALA was used as the substrate, significant amounts of ketone (13-Oxo-OTrE, RT 10.04), coeluting with 13-HPOTrE (RT 9.91), were detected at higher enzyme concentrations (≥6 μg/mL) (Fig. 4).

The chromatograms in Fig. 3 show that increasing the enzyme concentration from 3 to 9 μg/mL decreased substrate levels while increasing the formation of epoxy alcohols across all substrates tested. These findings indicate that a portion of the added Bt-LOX added, typically in its ferrous state (LOX–Fe^{2+}), reacts with FAHP (likely formed through autoxidation) and is oxidized to its ferric state. The ferric form of Bt-LOX exhibits dioxygenase activity, transforming PUFAs into FAHPs by reacting with oxygen. Elevated enzyme concentrations accelerate the dioxygenation reaction, which inherently increases oxygen consumption. Under these conditions, the accumulation of FAHPs and limited oxygen availability favor the HPI pathway, which converts FAHPs into epoxy alcohols (Fig. 1). HPI activity is more pronounced at higher enzyme concentrations due to the greater availability of ferrous Bt-LOX, which is required for this reaction. In contrast, at lower enzyme concentrations, a substantial portion of the enzyme is likely oxidized to the ferric state, thereby limiting its capacity to catalyze HPI activity.

In addition to epoxy alcohols, Bt-LOX also produces ketones from its HPI activity when using ALA and GLA as substrates at higher enzyme concentrations (≥6 μg/mL). Interestingly, ketones were barely detectable when LA was the substrate. It is possible that, when using LA, ketones were formed to some extent but remain too low to detect due to co-elution with FAHPs. This substrate-dependent variation in ketone production has also been observed with the fungal *Gaeumannomyces avenae* LOX [8]. Similar to Bt-LOX, this fungal LOX generates more ketone when ALA is used as the substrate compared to LA [8]. Consistent with the formation of epoxy alcohols, ketones production from ALA and GLA increases with enzyme concentration (Fig. 4). A similar trend of increased ketone formation with rising enzyme concentrations has also been reported for soybean LOX under anaerobic conditions [13].

In addition to FAHPs, epoxy alcohols, and ketones, other minor products were detected in the Bt-LOX reactions (Table S1). These include epoxy allylic hydroperoxides, likely produced through oxygen-dependent dissociation during enzyme activation, and hydroxy fatty acids, which represent the reduced forms of FAHPs.

3.2. Epoxy alcohol vs. ketone formation during the HPI cycle

The variation in the ratios of epoxy alcohol to ketone formation among different PUFAs may be influenced by the conformation of their hydroperoxides in the enzyme's active site. To better understand how the FAHPs interact with Bt-LOX during HPI catalysis, 13-HPODE, 13-αHPOTrE, and 13-γHPOTrE were docked in the substrate binding pocket of the Alphafold model of Bt-LOX. The obtained docking poses and parameters are listed in Table S2.

Even though each FAHP can adopt both head-first and tail-first orientations within the active site (Table S2), the docking pose most likely to represent the HPI reaction was selected based not only on the S-score and RMSD (<2 Å), but also on the proximity of the hydroperoxide group to the catalytic iron. The selected pose for 13-HPODE, which exclusively produces an epoxy alcohol, shows a tail-first orientation. In contrast, the selected poses for 13-αHPOTrE and 13-γHPOTrE, which yield both epoxy alcohols and ketones, exhibit head-first orientations. The selected poses, as shown in Fig. 5, indicate that the hydroperoxide group of each FAHP is positioned in close proximity to the iron (4.2–5.4 Å), facilitating the homolytic cleavage of the O–O bond to form an alkoxy radical intermediate, which may subsequently react to a ketone or cyclize into an epoxyallylic radical and form an epoxy alcohol through oxygen rebound (Fig. 1).

To rationalize the observed difference in products obtained, we performed QM/MM calculations to determine the relative energies of radical intermediates and products of 13-HPODE and 13-αHPOTrE in the substrate binding pocket of Bt-LOX (Fig. S6 and S7). As can be observed from Table 1, for both substrates, ketone and epoxy alcohol formation are highly exothermic. A clear difference can be observed, though, between the relative energies of the final products. Whereas epoxy alcohol formation seems to be thermodynamically preferred for

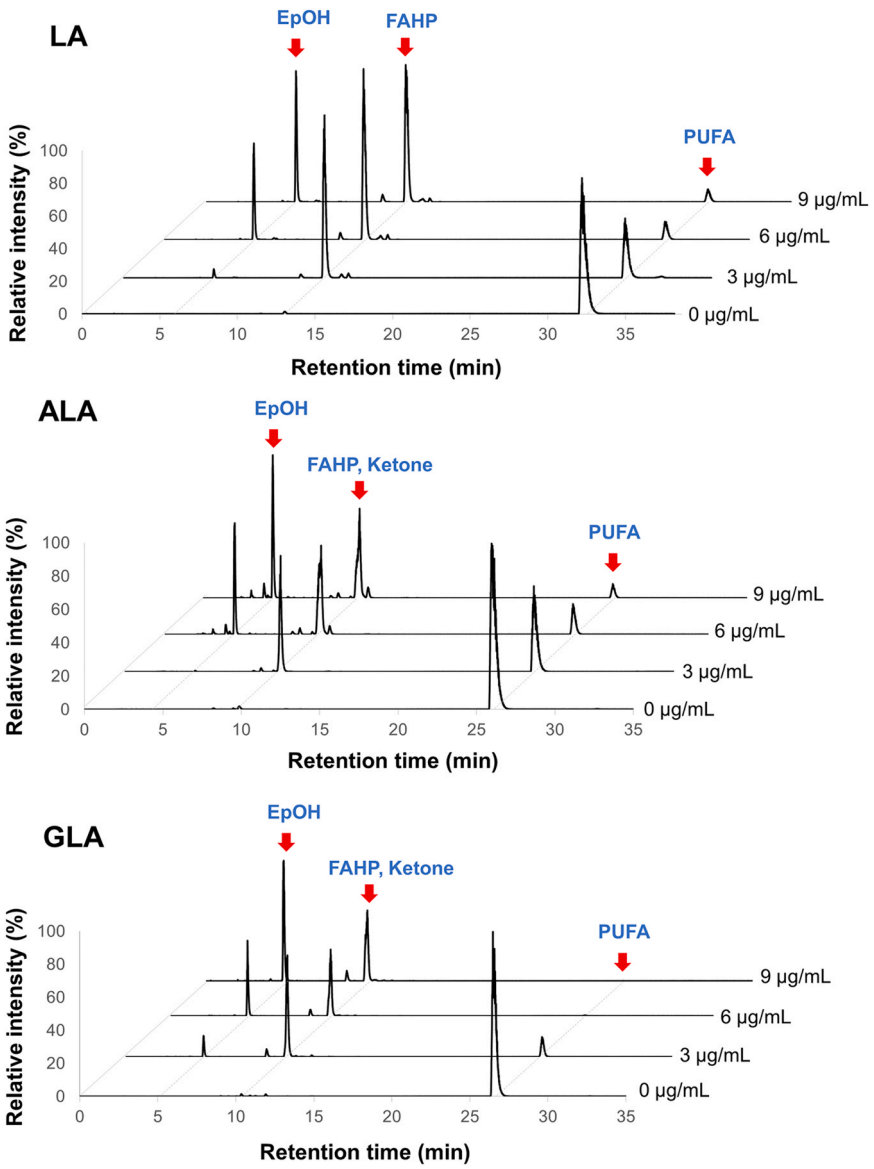

Fig. 3. Effect of enzyme concentrations (0, 3, 6, and 9 µg/mL) on the HPI activity of Bt-LOX using three different PUFA substrates: linoleic acid (LA; C18:2 $\Delta^{9Z,12Z}$), α-linolenic acid (ALA; C18:3 $\Delta^{9Z,12Z,15Z}$) and γ-linolenic acid (GLA; C18:3 $\Delta^{6Z,9Z,12Z}$). The enzyme and the substrates were dissolved in 100 mM Bis-Tris buffer pH 6.0 and the reaction mixtures were incubated for 30 min at 30 °C. The peaks of the polyunsaturated fatty acid (PUFA) and its corresponding fatty acid hydroperoxide (FAHP), ketone and epoxy alcohol (EpOH) are indicated in the figure with red arrows. The highest peak from the compared chromatograms was used as the reference of 100 %. Displayed chromatograms are representative chromatograms from experiments involving two biological replicates.

13-HPODE, ketone formation is thermodynamically favored in the case of 13-αHPOTrE. The clear thermodynamic preference of 13-HPODE to react to its epoxy alcohol derivative, corroborates with the observation that it hardly forms ketones. The fact that, despite a clear thermodynamic preference for ketone formation, 13-αHPOTrE reacts to a mixture of epoxy alcohols and ketones, indicates that other kinetic factors may also play a role in governing the selectivity. For 13-αHPOTrE, the H–O distance for a hydrogen atom transfer from the alkoxy radical to the Fe^{3+}–OH is 4.05 Å, whereas the C–O distance for the rebound reaction of the epoxyallylic radical is only 3.40 Å (Fig. S7), which indeed hints at a kinetic preference for epoxy alcohol formation. We note that detailed insights in such kinetic effects would require extensive reaction mechanism simulations, which is out of the scope of the current study.

3.3. Effect of reaction time on HPI activity

To evaluate the effect of reaction time on HPI product accumulation, the lowest enzyme concentration (3 µg/mL), at which low epoxy alcohol formation was observed, was used. The HPI activity of Bt-LOX was investigated at five time intervals: 0, 30, 60, 90, and 120 min. To confirm the stability of FAHPs under the experimental conditions, standard 13-HPOTrE was incubated without Bt-LOX under the same conditions as the samples for 0 and 120 min. No significant decomposition of 13-HPOTrE under these conditions was observed, except for a small amount (<2 %) converted to its reduced form, 13-HOTrE (Fig. S8). Enzymatic reaction products were analyzed using RP-UHPLC-PDA-HRMS, with the chromatograms presented in Fig. S9. The results indicated that increasing reaction times led to a decrease in PUFA levels and an increase in FAHP formation during the first 60–90 min. However, extending the incubation time to 120 min did not significantly affect PUFA levels or FAHP formation. Additionally, prolonged reaction times slightly elevated the formation of epoxy alcohols across all substrates. Nonetheless, at this low enzyme concentration, ketones were barely detectable for any of the substrates. Despite the presence of abundant

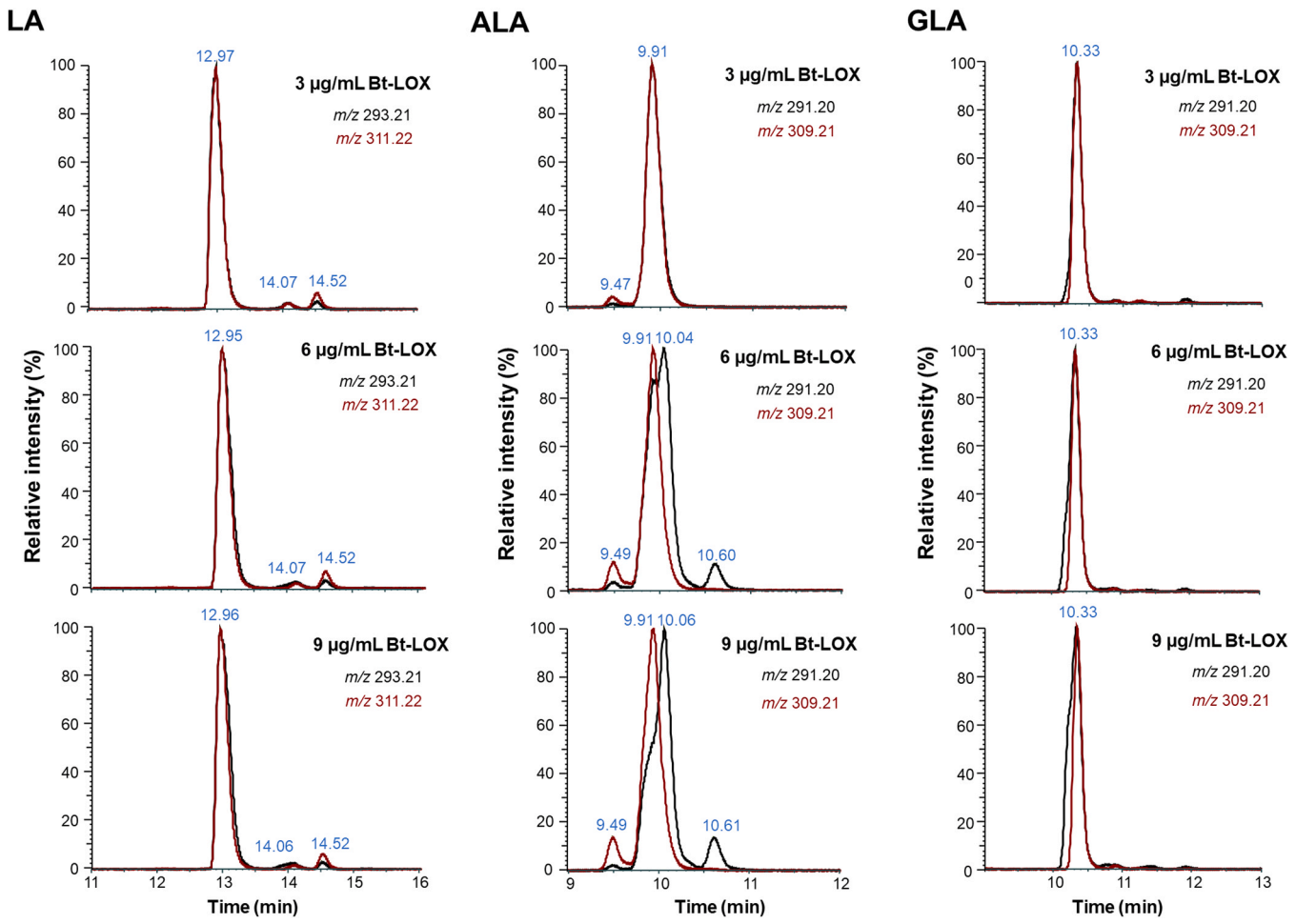

Fig. 4. Extracted ion chromatograms of the FAHP and ketone products obtained from different PUFAs (LA, ALA and GLA) by the reaction of Bt-LOX. Red lines indicate the *m/z* value of FAHPs while black lines indicate the *m/z* value of fatty acid ketones.

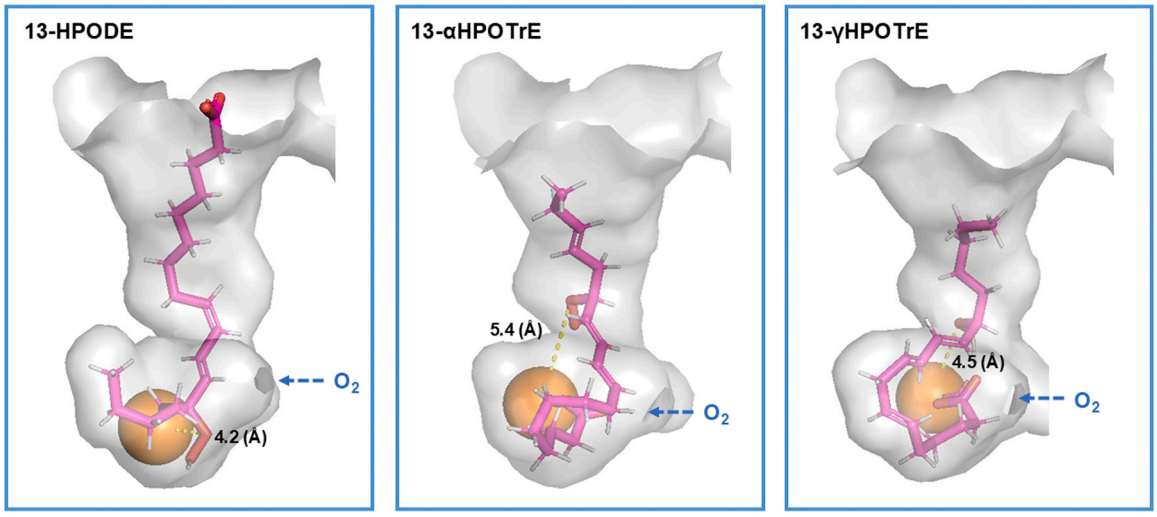

Fig. 5. Docking poses of three different FAHPs in the substrate-binding pocket of Bt-LOX. The 13-HPODE, 13-αHPOTrE, and 13-γHPOTrE are FAHPs derived from LA, ALA, and GLA, respectively. The three-dimensional structure of Bt-LOX was modeled using AlphaFold2. The position of the iron (shown as an orange sphere) was docked to the enzyme's active site prior the docking of FAHPs. The FAHPs (shown as magenta stick) were docked to the substrate binding pocket (shown in light grey) using MOE 2022.02. The directions of oxygen insertion from the putative oxygen channel are indicated as blue-dashes line arrows. The distances between the hydroperoxide group and the iron are shown as yellow dashed lines.

Table 1
Relative energies (kcal/mol) of the radical intermediates and final products of the hydroperoxide isomerase activity of Bt-LOX, as determined using QM/MM calculations. The energy of the alkoxy radical is defined as 0.

	13-HPODE	13-αHPOTrE
Alkoxy radical	0.0	0.0
Epoxyallylic radical	−30.5	−52.7
Epoxy alcohol	−106.7	−90.4
Ketone	−89.4	−110.0

FAHPs, epoxy alcohol production did not significantly increase over time, apparently due to enzyme inactivation after the first 60 min of incubation (Fig. S10). It is possible that the produced FAHPs inhibit and inactivate the enzyme, as certain FAHPs have been reported to irreversibly inhibit 5-LOX from guinea pig and soybean LOX-1 [29–32]. Although the exact mechanisms of this inactivation process remain unclear, it has been proposed that unstable radical intermediates generated during the iron atom-catalyzed cleavage of the hydroperoxide group, i.e. alkoxy radicals or epoxy radicals, may be responsible for the enzyme's inactivation [30,32].

3.4. Effect of oxygen level on HPI activity

During the enzyme activation, oxygen induces the dissociation of radical intermediates leading to generation of ferric enzyme species that are active for dioxygenase activity [5], while HPI activity is often associated with anaerobic or oxygen-limited conditions [5,7,13]. Therefore, modulating the oxygen level was hypothesized to direct the reaction pathway, either to dioxygenase or HPI activity. To study the impact of the oxygen level, the HPI activity of Bt-LOX was investigated under O_2-saturated and O_2-limited conditions. The reaction products were analyzed using RP-UHPLC-PDA-HRMS, and the chromatograms are shown in Fig. 6. The results showed that under O_2-saturated conditions, no formation of epoxy alcohols and ketones from both LA and ALA occurred. In contrast, under O_2-limited conditions, significant amounts of epoxy alcohols and ketones were formed from both LA and ALA.

Zoomed-in RP-UHPLC-HRMS and UV chromatograms highlighting FAHP formation under O_2-saturated conditions and ketone formation under O_2-limited conditions are shown in Fig. 7. Under O_2-saturated conditions, peaks corresponding to the MS chromatograms of FAHPs exhibit absorbance at 234 nm but not at 282 nm, indicating the presence of a conjugated diene moiety without a ketone group, confirming these peaks as FAHPs. In contrast, under O_2-limited conditions, peaks in the MS chromatograms of ketones show absorbance at both 234 nm and 282 nm, confirming their identity as ketones. When ALA was used as the substrate under O_2-limited conditions, a minor amount of FAHP, appearing as a shoulder peak at RT 9.82 and coeluting with its corresponding ketone, was still detected (Fig. 7).

The absence of epoxy alcohols and ketones in O_2-saturated environments highlights the critical role of oxygen in steering the Bt-LOX reaction toward dioxygenation while suppressing the HPI pathway (Fig. 8). Previous studies with eukaryotic LOXs suggested that, during the LOX activation process, molecular oxygen readily reacts with alkoxy and epoxy allylic radicals, promoting the activation of the enzyme to its free ferric form thus inhibiting HPI cycling (Fig. 8) [5,33,34]. On the other hand, the significant formation of epoxy alcohols and ketones under O_2-limited conditions point to an enhancement of the HPI activity of Bt-LOX (Fig. 8).

It appears that the low residual oxygen levels initially present during the Bt-LOX reactions support the conversion of PUFAs into their corresponding FAHPs, which are subsequently transformed into epoxy alcohols and ketones due to pronounced HPI activity in an oxygen-limited

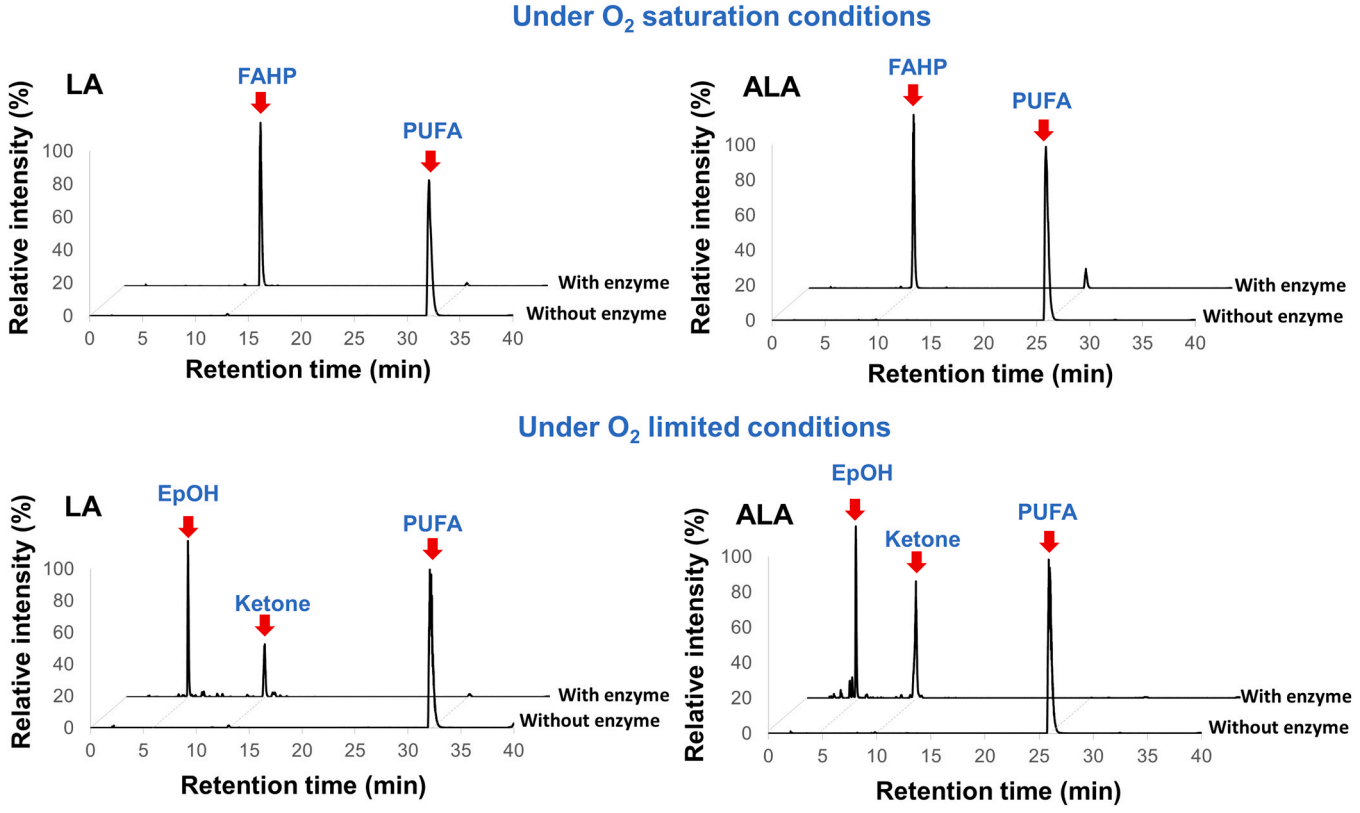

Fig. 6. Effect of oxygen level on the HPI activity of Bt-LOX using two different PUFA substrates: linoleic acid (LA; C18:2 $\Delta^{9Z,12Z}$) and α-linolenic acid (ALA; C18:3 $\Delta^{9Z,12Z,15Z}$). The substrate and 9 μg/mL enzyme were dissolved in 100 mM Bis-Tris buffer pH 6.0 and the reaction mixtures were incubated for 60 min at 30 °C under 100 mL/min O_2 or N_2 flow. The peaks of the polyunsaturated fatty acid (PUFA) and its corresponding fatty acid hydroperoxide (FAHP), epoxy alcohol (EpOH) and ketone are indicated in the figure with red arrows. Displayed chromatograms are representative of identical chromatograms from three biological replicates.

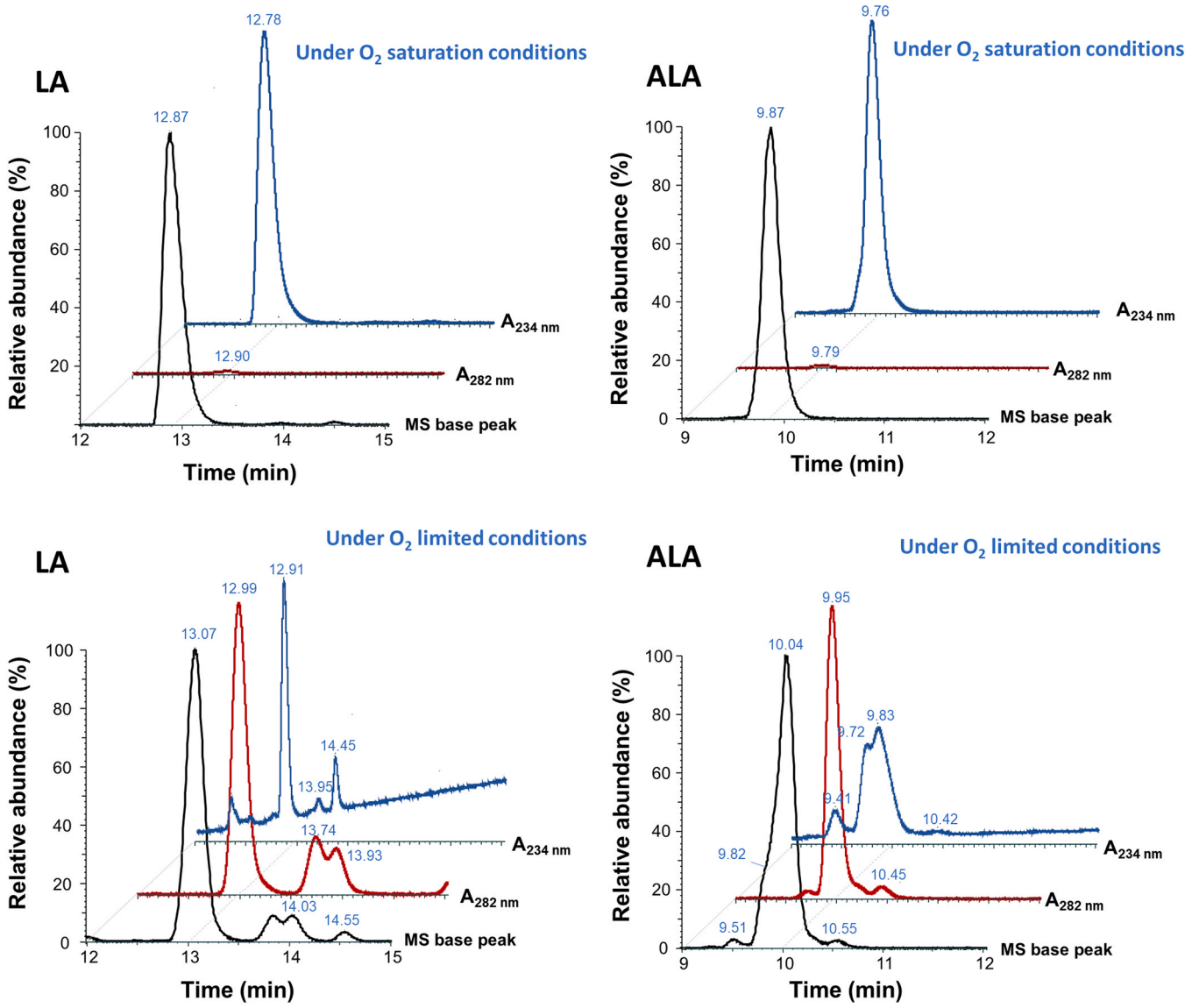

Fig. 7. Reverse phase UHPLC-MS and UV chromatograms of enzymatic product of Bt-LOX using LA (left) and ALA (right) under O_2-saturated and O_2-limited conditions. The MS chromatograms are indicated by black line, while $UV_{282\ nm}$ chromatograms are indicated by red line and $UV_{234\ nm}$ chromatograms are indicated by blue line. The presence of FAHPs under O_2-saturated conditions is confirmed by the UV absorbance at 234 nm indicating the presence of conjugated diene moiety, while the presence of ketones under O_2-limited conditions is confirmed by the UV absorbance at 282 nm. Note that ketones also contain a conjugated diene moiety, which absorbs at 234 nm.

environment. This observation aligns with previous reports suggesting that restricted oxygen access within the active site promotes HPI activity [5,8]. These findings demonstrate that controlling oxygen levels provides a means to modulate the Bt-LOX activity, directing it toward either dioxygenase or HPI activity. Such modulation has the potential to expand the enzyme's applications in various fields. Notably, under O_2-limited conditions, we successfully demonstrated the transformation of PUFAs into epoxy alcohols and ketones. This represents a significant advancement in PUFA derivatization, enabling both dioxygenase- and HPI-catalyzed reactions to occur under controlled conditions.

4. Conclusions

This study presents the first report of pronounced HPI activity in a bacterial LOX, marking a significant advancement in the field of LOX catalysis. Oxygen levels emerged as a key factor in modulating Bt-LOX activity: O_2-saturated conditions suppressed HPI activity, whereas O_2-limited conditions significantly enhanced it, enabling the efficient production of epoxy alcohols and ketones. The variation in the ratios of epoxy alcohol to ketone formation among different PUFAs is most likely influenced by the ease of hydroxy group rebound from the LOX–Fe^{3+}–OH complex to the radical intermediates formed during the HPI cycle. Molecular dynamic simulations can be used to clarify further the exact mechanisms. The ability of Bt-LOX to catalyze the formation of regiospecific FAHPs, along with their epoxy alcohol and ketone derivatives, underscores its potential as a versatile biocatalyst. These findings provide a foundation for innovative strategies in PUFA derivatization and highlight the promise of Bt-LOX for applications in biocatalysis and green chemistry.

CRediT authorship contribution statement

Guanna Li: Writing – review & editing, Methodology. **Roelant Hilgers:** Writing – review & editing, Methodology, Investigation, Formal analysis. **Ruth Chrisnasari:** Writing – review & editing, Writing – original draft, Visualization, Methodology, Investigation, Formal

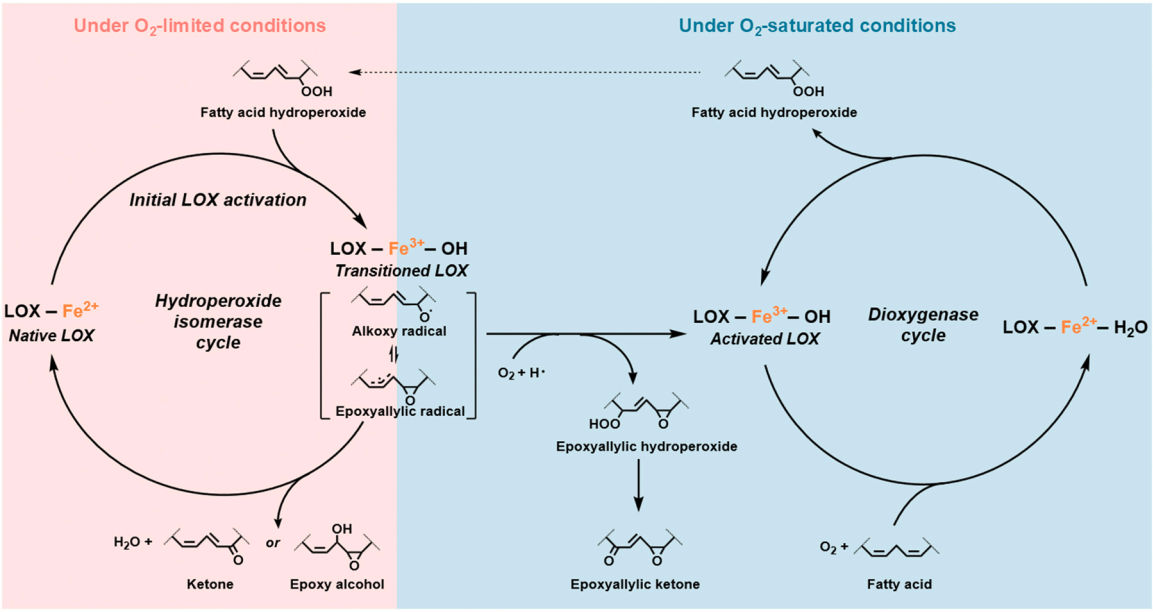

Fig. 8. Initial LOX activation and its subsequent dioxygenase or hydroperoxide isomerase (HPI) activity. Activation of the non-heme iron cofactor of LOX by FAHP (generated through auto-oxidation) leads to the formation of an alkoxy or epoxy-allylic radical intermediate. In the presence of oxygen, these radical intermediates dissociate via an oxygen-dependent pathway to form an epoxy-allylic hydroperoxide, which is subsequently transformed into an epoxy-allylic ketone. The free ferric enzyme then catalyzes a dioxygenase reaction, converting PUFA into FAHP. Under O_2-saturated conditions, both the oxygen-dependent dissociation of the radical intermediates and the dioxygenase reaction become more pronounced. Conversely, under O_2-limited conditions, the radical intermediate can be transformed into an epoxy alcohol or ketone by HPI activity, with the iron in LOX being regenerated to its ferrous state upon product release. When continuous regeneration of the ferrous enzyme occurs due to HPI activity, the FAHP produced by dioxygenase activity can enter the HPI cycle and be further transformed into either an epoxy alcohol or ketone (indicated by a dashed arrow).

analysis, Conceptualization. **Tom A. Ewing:** Writing – review & editing, Supervision, Conceptualization. **Marie Hennebelle:** Writing – review & editing, Supervision, Conceptualization. **van Berkel Willem J. H.:** Writing – review & editing, Supervision. **Jean-Paul Vincken:** Writing – review & editing, Supervision.

Funding

The PhD study of R. Chrisnasari was supported by the Indonesian Endowment Fund for Education (LPDP, grant number 0006605/BIO/D/BUDI-2019).

Declaration of Competing Interest

The authors declare that they have no known competing financial interests or personal relationships that could have appeared to influence the work reported in this paper.

Acknowledgement

The authors gratefully acknowledge Mark Sanders for his assistance during UHPLC-MS method development and Dr. Daan van Vliet for his support in setting up the greenhouse and parallel synthesizer. Part of the results presented were obtained using a Thermo Scientific Q Exactive Focus Orbitrap MS system, owned by Shared Research Facilities-WUR and subsidized by the province of Gelderland, The Netherlands.

Appendix A. Supporting information

Supplementary data associated with this article can be found in the online version at doi:10.1016/j.enzmictec.2025.110709.

Data availability

Data will be made available on request.

References

[1] J.J.M.C. de Groot, G.J. Garssen, G.A. Veldink, J.F.G. Vliegenthart, J. Boldingh, M. R. Egmond, On the interaction of soybean lipoxygenase-1 and 13-L-hydroperoxy-linoleic acid, involving yellow and purple coloured enzyme species, FEBS Lett. 56 (1975) 50–54, https://doi.org/10.1016/0014-5793(75)80109-8.
[2] M.J. Schilstra, G.A. Veldink, J.F.G. Vliegenthart, Kinetic analysis of the induction period in lipoxygenase catalysis, Biochemistry 32 (1993) 7686–7691, https://doi.org/10.1021/bi00081a012.
[3] M.J. Schilstra, G.A. Veldink, J. Verhagen, J.F.G. Vliegenthart, Effect of lipid hydroperoxide on lipoxygenase kinetics, Biochemistry 31 (1992) 7692–7699, https://doi.org/10.1021/bi00148a033.
[4] M.J. Schilstra, G.A. Veldink, J.F.G. Vliegenthart, The dioxygenation rate in lipoxygenase catalysis is determined by the amount of Iron(III) lipoxygenase in solution, Biochemistry 33 (1994) 3974–3979, https://doi.org/10.1021/bi00179a025.
[5] Y. Zheng, A.R. Brash, On the role of molecular oxygen in lipoxygenase activation: comparison and contrast of epidermal lipoxygenase-3 with soybean lipoxygenase-1, J. Biol. Chem. 285 (2010) 39876–39887, https://doi.org/10.1074/jbc.M110.180794.
[6] Z. Yu, C. Schneider, W.E. Boeglin, L.J. Marnett, A.R. Brash, The lipoxygenase gene ALOXE3 implicated in skin differentiation encodes a hydroperoxide isomerase, PNAS 100 (2003) 9162–9167, https://doi.org/10.1073/pnas.1633612100.
[7] G.J. Garssen, G.A. Veldink, J.F.G. Vliegenthart, J. Boldingh, The formation of threo-11-hydroxy-*trans*-12: 13-epoxy-9-*cis*-octadecenoic acid by enzymic isomerisation of 13-*l*-hydroperoxy-9-*cis*,11-*trans*-octadecadienoic acid by soybean lipoxygenase-1, Eur. J. Biochem 62 (1976) 33–36, https://doi.org/10.1111/j.1432-1033.1976.tb10094.x.
[8] M. Cristea, E.H. Oliw, A G316A mutation of manganese lipoxygenase augments hydroperoxide isomerase activity: mechanism of biosynthesis of epoxyalcohols, J. Biol. Chem. 281 (2006) 17612–17623, https://doi.org/10.1074/jbc.M510311200.
[9] C.T. Hou, Biotechnology for fats and oils: new oxygenated fatty acids, N. Biotechnol. 26 (2009) 2–10, https://doi.org/10.1016/j.nbt.2009.05.001.
[10] A. Riera, M. Moreno, Synthetic applications of chiral unsaturated epoxy alcohols prepared by Sharpless asymmetric epoxidation, Molecules 15 (2010) 1041–1073, https://doi.org/10.3390/molecules15021041.

[11] A.R. Brash, Z. Yu, W.E. Boeglin, C. Schneider, The hepoxilin connection in the epidermis, FEBS J. (2007) 3494–3502, https://doi.org/10.1111/j.1742-4658.2007.05909.x.
[12] J.U. An, Y.S. Song, K.R. Kim, Y.J. Ko, D.Y. Yoon, D.K. Oh, Biotransformation of polyunsaturated fatty acids to bioactive hepoxilins and trioxilins by microbial enzymes, Nat. Commun. 9 (2018) 1–10, https://doi.org/10.1038/s41467-017-02543-8.
[13] G.J. Garssen, J.F.G. Vliegenthart, J. Boldingh, An anaerobic reaction between lipoxygenase, linoleic acid and its hydroperoxides, Biochem. J. 122 (1971) 327–332, https://doi.org/10.1042/bj1220327.
[14] Y. Zheng, A.R. Brash, Dioxygenase activity of epidermal lipoxygenase-3 unveiled: typical and atypical features of its catalytic activity with natural and synthetic polyunsaturated fatty acids, J. Biol. Chem. 285 (2010) 39866–39875, https://doi.org/10.1074/jbc.M110.155374.
[15] J.U. An, B.J. Kim, S.H. Hong, D.K. Oh, Characterization of an omega-6 linoleate lipoxygenase from *Burkholderia thailandensis* and its application in the production of 13-hydroxyoctadecadienoic acid, Appl. Microbiol Biotechnol. 99 (2015) 5487–5497, https://doi.org/10.1007/s00253-014-6353-8.
[16] R. Chrisnasari, M. Hennebelle, J.-P. Vincken, W.J.H. van Berkel, T.A. Ewing, Bacterial lipoxygenases: biochemical characteristics, molecular structure and potential applications, Biotechnol. Adv. 61 (2022) 108046, https://doi.org/10.1016/j.biotechadv.2022.108046.
[17] R. Chrisnasari, M. Hennebelle, K.A. Nguyen, J.-P. Vincken, W.J.H. van Berkel, T. A. Ewing, Engineering the substrate specificity and regioselectivity of *Burkholderia thailandensis* lipoxygenase, N. Biotechnol. 84 (2024) 64–76, https://doi.org/10.1016/j.nbt.2024.09.007.
[18] M.M. Bradford, A rapid and sensitive method for the quantitation of microgram quantities of protein utilizing the principle of protein-dye binding, Anal. Biochem 72 (1976) 248–254.
[19] R. Chrisnasari, T.A. Ewing, R. Hilgers, W.J.H. van Berkel, J.-P. Vincken, M. Hennebelle, Versatile ferrous oxidation–xylenol orange assay for high-throughput screening of lipoxygenase activity, Appl. Microbiol Biotechnol. 108 (2024) 266, https://doi.org/10.1007/s00253-024-13095-5.
[20] J.U. An, S.H. Hong, D.K. Oh, Regiospecificity of a novel bacterial lipoxygenase from *Myxococcus xanthus* for polyunsaturated fatty acids, Biochim Biophys. Acta Mol. Cell Biol. Lipids 1863 (2018) 823–833, https://doi.org/10.1016/j.bbalip.2018.04.014.
[21] F.P. Corongiu, S. Bani, Detection of conjugated dienes by second derivative ultraviolet spectrophotometry, Methods Enzym. (1941) 303–310, https://doi.org/10.1016/s0076-6879(94)33033-6.
[22] P.B.M.C. Derogis, A.B. Chaves-Fillho, S. Miyamoto, Characterization of hydroxy and hydroperoxy polyunsaturated fatty acids by mass spectrometry. Advances in Experimental Medicine and Biology, Springer New York LLC, 2019, pp. 21–35, https://doi.org/10.1007/978-3-030-11488-6_2.
[23] P.B.M.C. Derogis, F.P. Freitas, A.S.F. Marques, D. Cunha, P.P. Appolinário, The development of a specific and sensitive LC-MS- based method for the detection and quantification of hydroperoxy- and hydroxydocosahexaenoic acids as a tool for lipidomic analysis, PLoS One 8 (2013) 77561, https://doi.org/10.1371/journal.pone.0077561.
[24] J. Jumper, R. Evans, A. Pritzel, T. Green, M. Figurnov, O. Ronneberger, K. Tunyasuvunakool, R. Bates, A. Žídek, A. Potapenko, A. Bridgland, C. Meyer, S.A. A. Kohl, A.J. Ballard, A. Cowie, B. Romera-Paredes, S. Nikolov, R. Jain, J. Adler, T. Back, S. Petersen, D. Reiman, E. Clancy, M. Zielinski, M. Steinegger, M. Pacholska, T. Berghammer, S. Bodenstein, D. Silver, O. Vinyals, A.W. Senior, K. Kavukcuoglu, P. Kohli, D. Hassabis, Highly accurate protein structure prediction with AlphaFold, Nature 596 (2021) 583–589, https://doi.org/10.1038/S41586-021-03819-2.
[25] J. Abramson, J. Adler, J. Dunger, R. Evans, T. Green, A. Pritzel, O. Ronneberger, L. Willmore, A.J. Ballard, J. Bambrick, S.W. Bodenstein, D.A. Evans, C.C. Hung, M. O'Neill, D. Reiman, K. Tunyasuvunakool, Z. Wu, A. Žemgulytė, E. Arvaniti, C. Beattie, O. Bertolli, A. Bridgland, A. Cherepanov, M. Congreve, A.I. Cowen-Rivers, A. Cowie, M. Figurnov, F.B. Fuchs, H. Gladman, R. Jain, Y.A. Khan, C.M. R. Low, K. Perlin, A. Potapenko, P. Savy, S. Singh, A. Stecula, A. Thillaisundaram, C. Tong, S. Yakneen, E.D. Zhong, M. Zielinski, A. Žídek, V. Bapst, P. Kohli, M. Jaderberg, D. Hassabis, J.M. Jumper, Accurate structure prediction of biomolecular interactions with AlphaFold 3, Nature 630 (2024) 493–500, https://doi.org/10.1038/s41586-024-07487-w.
[26] M.J. Frisch, G.W. Trucks, H.B. Schlegel, G.E. Scuseria, M.A. Robb, J.R. Cheeseman, G. Scalmani, V. Barone, G.A. Petersson, H. Nakatsuji, X. Li, M. Caricato, A.V. Marenich, J. Bloino, B.G. Janesko, R. Gomperts, B. Mennucci, H.P. Hratchian, J.V. Ortiz, A.F. Izmaylov, J.L. Sonnenberg, D. Williams-Young, F.; Ding, F. Lipparini, F. Egidi, J. Goings, B. Peng, A. Petrone, T. Henderson, D. Ranasinghe, V.G. Zakrzewski, J. Gao, N. Rega, G. Zheng, W. Liang, M. Hada, M. Ehara, K. Toyota, R.; Fukuda, J. Hasegawa, M. Ishida, T. Nakajima, Y. Honda, O. Kitao, H. Nakai, T. Vreven, K. Throssell, J.A., Jr. Montgomery, J.E. Peralta, F. Ogliaro, M.J. Bearpark, J.J. Heyd, E.N. Brothers, K.N. Kudin, V.N.; Staroverov, T.A. Keith, R. Kobayashi, J. Normand, K. Raghavachari, A.P. Rendell, J.C. Burant, S.S.; Iyengar, J. Tomasi, M. Cossi, J.M. Millam, M. Klene, C. Adamo, R. Cammi, J.W. Ochterski, R.L. Martin, K. Morokuma, O. Farkas, J.B. Foresman, D.J. Fox, Gaussian 16, Revision C.01, (2016).
[27] T.M. Cheesbrough, B. Axelrod, Determination of the spin state of iron in native and activated soybean lipoxygenase 1 by paramagnetic susceptibility, Biochemistry 22 (1983) 3837–3840, https://doi.org/10.1021/bi00285a019.
[28] W.R. Dunham, R.T. Carrol, J.F. Thompson, R.H. Sands, M.O. Funk, The initial characterization of the iron environment in lipoxygenase by Mössbauer spectroscopy, Eur. J. Biochem 190 (1990) 611–617, https://doi.org/10.1111/j.1432-1033.1990.tb15616.x.
[29] D. Aharony, D.G. Redkar–brown, S.J. Hubbs, R.L. Stein, Kinetic studies on the inactivation of 5-lipoxygenase by 5(*S*)-hydroperoxyeicosatetraenoic acid, Prostaglandins 33 (1987) 85–100, https://doi.org/10.1016/0090-6980(87)90307-8.
[30] M.R. Kim, D.-E. Sok, Irreversible inhibition of soybean lipoxygenase-I by hydroperoxy acids as substrates, Arch. Biochem Biophys. 288 (1991) 270–275, https://doi.org/10.1016/0003-9861(91)90194-n.
[31] C.H. Reynolds, Inactivation of soybean lipoxygenase by lipoxygenase inhibitors in the presence of 15-hydroperoxyeicosatetraenoic acid, Biochem Pharm. 37 (1988) 4531–4537, https://doi.org/10.1016/0006-2952(88)90669-7.
[32] W.F. Nieuwenhuizen, A. Van Der Kerk-Van Hoof, J.H. Van Lenthe, R.C. Van Schaik, K. Versluis, G.A. Veldink, J.F.G. Vliegenthart, Lipoxygenase is irreversibly inactivated by the hydroperoxides formed from the enynoic analogues of linoleic acid, Biochemistry 36 (1997) 4480–4488, https://doi.org/10.1021/bi962956l.
[33] I. Ivanov, J. Saam, H. Kuhn, H.G. Holzhütter, Dual role of oxygen during lipoxygenase reactions, FEBS J. 272 (2005) 2523–2535, https://doi.org/10.1111/j.1742-4658.2005.04673.x.
[34] E. Faillace, V. Brunini-Bronzini de Caraffa, C. Gambotti, L. Berti, J. Maury, S. Vincenti, Optimizing the second step of the biocatalytic process for green leaf volatiles production: synthesis by soybean 13-lipoxygenase of 13-hydroperoxides from hydrolyzed hempseed oil, Biocatal. Agric. Biotechnol. 65 (2025), https://doi.org/10.1016/j.bcab.2025.103548.